Terahertz Spectroscopy: System and Sensitivity Considerations

Heinz-Wilhelm Hübers, Maurice F. Kimmitt, Norihisa Hiromoto, and Erik Bründermann

(Invited Paper)

***Abstract*—Terahertz spectroscopy is a backbone method in many areas of research. We have analyzed typically employed THz spectroscopy systems and their sensitivity in a general comparative approach. Recent progress to reduce the data acquisition time by frequency multiplexing using a spectrometer with a THz quantum cascade laser is described. The performance of a spectrometer using a pulsed Ge THz laser with a few μs long integration time and recent progress to modulate the laser current within such a short pulse are presented. We also investigate the origin of random errors in intensity spectra of a THz TDS with the goal to identify common error sources in TDS systems to allow reduction of the total measurement time.**

***Index Terms*—Terahertz germanium laser, terahertz quantum cascade laser, terahertz spectroscopy, terahertz time-domain spectrometer.**

I. Introduction

SPECTROSCOPY at terahertz (THz) frequencies is a very powerful tool for a wide range of applications [1], [2]. One example is high resolution spectroscopy of molecules and atoms. Besides information on the species itself, important information on Doppler and pressure broadening can be obtained from THz spectra. THz spectroscopy of astronomical sources and planetary atmospheres including the Earth is another important application and last but not least spectroscopy of chemical compounds such as pharmaceuticals or explosives is gaining rapid interest because it is of relevance for biomedicine and security.

When designing a spectrometer for a particular application it is important to keep in mind that ultimately it is not the performance of single components, but the overall performance of the whole spectrometer, which is important. Single components may have an exceptional performance but, if the system design does not take into account the interplay between the various components, the spectrometer will not be optimized. Therefore, a few system aspects relevant for THz spectrometers will be discussed in this section. In general the optimization goal is to obtain very high quality data, i.e., data with a significant signal-to-noise (S/N)-ratio in a given data acquisition time. This is not only a question of data quality but also a question of economy, for example, to make the most efficient use of expensive observing time on a satellite or in commercial applications where "time is money". It should be noted that the data acquisition time is not necessarily identical to the integration time, which is usually stated in equations describing the sensitivity of a system. Obviously for spectrometers operating in a pulsed mode the integration time is much shorter than the data acquisition time. For example, a time domain spectrometer has a typical duty cycle in the order of 10^{-4} and a spectrometer with a pulsed p-type Ge laser has a duty cycle of up to 0.1.

Before discussing some real spectrometers it is useful to consider the sensitivity limits. We will restrict this discussion to absorption measurements. Reflectivity measurements can be treated in an analogue way. A typical spectrometer consists of a radiation source, an absorption cell or a holder with the sample under investigation, a detector, and optical elements. The THz source emits radiation with power P_{S} at a frequency ν in a frequency band $\Delta\nu$. The radiation is transmitted through an absorption cell, which is filled with a gas at a particular pressure. Alternatively a solid sample can replace the absorption cell. The transmitted radiation impinges on a detector and generates an output voltage or current. The THz source is modulated by an appropriate method, and the output signal of the detector is measured with reference to the modulation frequency by a lock-in technique. Frequently employed sources are backward wave oscillators (BWOs) [3], [4], harmonic generators based on frequency multiplication [5], or sources based on photomixing of two infrared or near-infrared lasers [6]. These sources are typically combined with pyroelectric detectors, Golay cell detectors, or liquid helium cooled devices such as InSb bolometers, Si composite bolometers, or Ge:Ga photoconductive detectors. Although somewhat different from the absorption spectrometer with frequency tunable, narrow-band, and continuous wave (cw) sources, time domain spectrometers (TDS) and Fourier transform spectrometers (FTS) can be considered in a similar way. In the case of TDS a photomixer or a

Manuscript received March 28, 2011; revised June 06, 2011; accepted June 07, 2011. Date of current version August 31, 2011.

E. Bründermann is with the Shizuoka University, Hamamatsu, Japan, and also with the Ruhr-Universität Bochum, 44780 Bochum, Germany (e-mail: erik.bruendermann@rub.de).

H.-W. Hübers is with the Deutsches Zentrum für Luft- und Raumfahrt e. V. and Technische Universität Berlin, 12489 Berlin, Germany (e-mail: heinz-wilhelm.huebers@dlr.de).

M. F. Kimmitt is with the Physics Centre, University of Essex, Colchester CO4 3SQ, U.K. (e-mail: m.kimmitt292@btinternet.com).

N. Hiromoto is with the Graduate School of Science and Technology, Shizuoka University, Hamamatsu, Shizuoka 432-8011, Japan (e-mail: dnhirom@ipc.shizuoka.ac.jp).

Color versions of one or more of the figures in this paper are available online at http://ieeexplore.ieee.org.

Digital Object Identifier 10.1109/TTHZ.2011.2159877

TABLE I
TYPICAL PERFORMANCE VALUES OF A VARIETY OF THZ SPECTROMETERS.

Source/spectrometer	Cw BWO	Cw multiplier	Cw QCL	Cw photomixer	p-type Ge	TDS	FTS
Frequency coverage (THz)	0.1–1.5	0.1–2.6	1–5	0.1–2	1–4	0.1–5 [1)]	0.3–20 [2)]
Bandwidth (THz)	10–20% of c.f.[3)]	10–20% of c.f.[3)]	10–20% of c.f.[3)]	0.1–2	1–4 tunable	0.1–5 [1)]	0.3–20 [2)]
Spectral resolution (MHz)	< 1 [4)]	< 1 [4)]	< 1 [4)]	> 1	< 1 [5)]	3000 [6)]	3000 [6)]
Spectral brightness (mW/MHz)	20–0.01 [7)]	1–0.01 [7)]	0.1–100 [7)]	10^{-3}–10^{-7}	0.1–1000 [8)]	2×10^{-19} [9)]	10^{-14}
Duty cycle [10)]	1	1	1	1	10^{-4}–0.1	10^{-4}	1
Detector NEP (W/$\sqrt{\text{Hz}}$)	10^{-8}–10^{-13} [11)]	10^{-8}–10^{-13} [11)]	10^{-8}–10^{-13} [11)]	10^{-14}	10^{-13}	10^{-16}	10^{-8}–10^{-13} [11)]

The listed values are representative but might be different - easily up to one order of magnitude - when a particular spectrometer is considered (data are from various sources).
1) The upper frequency limit is determined by the type of emitter/detector, in this case a photoconductive switch is assumed.
2) The upper frequency limit of the FTS is limited by the detector which is assumed to be a Si bolometer.
3) These sources cannot cover the whole frequency range with a single device. The given bandwidths are typical values where the output power and spectral brightness of the source does not fall below 10% of its peak value; c.f.: center frequency of a single device.
4) The spectral resolution is limited by the linewidth of the source.
5) The spectral resolution is limited by the laser pulse length which results in a Fourier-limited linewidth.
6) Spectral resolution which is achievable with a commonly used delay line length of several cm.
7) The first value corresponds to the lowest frequency and the second to the highest operating frequency given in the first row.
8) The highest value can be achieved for an external single mode resonator in a pulse mode with a low duty cycle less than 10^{-4}.
9) Time-averaged spectral brightness.
10) Modulation applied for lock-in detection is not taken into account.
11) First value: typical for room-temperature detectors; second value: typical for liquid helium cooled detectors.

nonlinear crystal is the source of THz radiation and the detector is also a photomixer or an electro-optic crystal. The time-gated, coherent detection in TDS reduces significantly the noise. In the case of an FTS a globar, a mercury arc lamp, incoherent or coherent terahertz radiation from an electron storage ring is the source while for detection the same devices are used as in cw spectroscopy. A comparison of different spectrometers is given in Table I. It should be noted that the values given in Table I are to some extent simplified to facilitate comparison. Nevertheless, they represent the relative order of magnitude. For a detailed study of the trade-offs between the different techniques a more detailed comparison needs to be undertaken which is beyond the scope of this article.

This paper is organized as follows: In Section II some general sensitivity considerations are discussed. The following Section III describes a cw THz spectrometer with a THz quantum cascade laser (QCL) and recent progress on the development to reduce the total measurement time by frequency multiplexing. In Sections IV and V spectrometers based on pulsed sources are discussed. The performance of a spectrometer with a pulsed Ge THz laser using short integration times of a few μs and recent progress to modulate the laser current within such a short pulse are discussed. Finally, Section V is devoted to random errors in intensity spectra of a specific THz TDS with the goal to distinguish systematic and random error sources common in TDS systems and to identify the instrument function to be able to predict sample absorption with its statistical errors in a reduced total measurement time.

II. SENSITIVITY CONSIDERATIONS

If the absorption is described by the Lambert-Beer law the change of power ΔP on the detector caused by a small absorption is given by $\Delta P = P_{\text{S}}(1 - \exp(-\alpha L)) \approx \alpha L P_{\text{S}}$. Here α is the absorption coefficient and L is the length of the absorption cell or the thickness of the sample under investigation. The minimum detectable change of power on the detector for a given source power is limited by the noise of the detector and therefore the minimum detectable absorption $\delta_{\min} = \alpha_{\min} L$ is given by the ratio of the detector NEP to the source power P_{S} per unit bandwidth. In the case of spectroscopy with a cw source lock-in amplification is usually employed. The lock-in amplifier converts an AC signal into a DC signal. This results in a factor of two power loss of the signal, while the NEP does not change. The minimum detectable absorption is further increased because the modulation of the signal must be taken into account. M is the modulation index of the detection scheme. Its value is between 0 (no modulation) and 1 (full modulation of the absorption feature). Taking this into account the minimum detectable absorption is obtained for a bandwidth B as [7]

$$\delta_{\min} = \frac{2}{M} \frac{\text{NEP}\sqrt{B}}{P_{\text{S}}}. \tag{1}$$

In Fig. 1 the minimum detectable absorption for different source-detector combinations is plotted. The curves are calculated according to (1) assuming an integration time of 1 s for a spectral resolution element. The spectral resolution is 1 MHz, except for TDS and FTS, where 3 GHz was assumed. A better spectral resolution with FTS and TDS is rarely accomplished because of the rather long and impractical mechanical delay lines (on the order of 100 m) necessary to realize a spectral resolution of 1 MHz. In the case of TDS it is possible to use non-mechanical, such as asynchronous optical sampling techniques which gives a better spectral resolution down to about 100 MHz [8]. For TDS an NEP of $10^{-16} W/\sqrt{\text{Hz}}$ [9] and for cw photomixing an NEP of $10^{-14} W/\sqrt{\text{Hz}}$ was used. A frequency-independent detector NEP of $10^{-12} W/\sqrt{\text{Hz}}$ is assumed for all other spectrometers. This NEP is a typical value for liquid helium cooled detectors. If a Golay cell detector or a pyroelectric detector is used the NEP and, correspondingly, the minimum detectable absorption increases according to (1).

The minimum detectable absorption increases approximately exponentially with increasing frequency for nearly all spectroscopic systems. This is caused by the exponential loss of source power which was assumed for simplicity. An exception is the

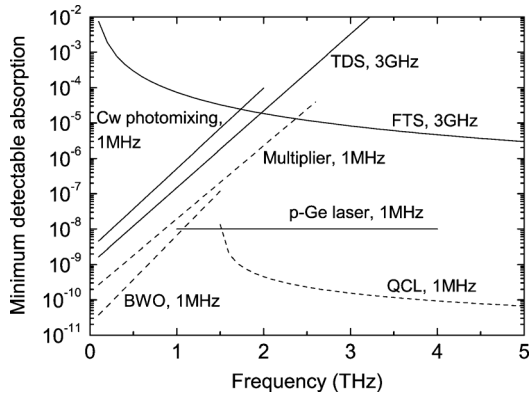

Fig. 1. Minimum detectable absorption for several spectrometers with different radiation sources as indicated by the labeling. The curves are calculated according to (1). Except for FTS and TDS (spectral resolution of 3 GHz) a spectral resolution of 1 MHz is assumed. A frequency-independent detector NEP of $10^{-12}W/\sqrt{\mathrm{Hz}}$ is assumed for all spectrometers except for TDS ($\mathrm{NEP} = 10^{-16}W/\sqrt{\mathrm{Hz}}$) and cw photomixing ($\mathrm{NEP} = 10^{-14}W/\sqrt{\mathrm{Hz}}$). For all cw spectrometers except for the cw photomixing lock-in detection with a modulation index of 0.3 was assumed. The dashed lines indicate spectrometers which cannot cover the whole frequency range with a single source.

QCL if it is used as a source. For QCLs the output power increases roughly linearly with frequency [10] which leads to an increasing spectrometer sensitivity at higher frequencies. Because of the rather large output power and narrow bandwidth of spectrometers with a QCL source they are potentially very sensitive in a portion of the THz region where only a few sensitive spectrometers exist. Similar to QCLs the source power of an FTS increases approximately linearly with frequency. It is worth noting that the loss in sensitivity toward lower frequencies in an FTS might be overcome when using coherent synchrotron radiation instead of a mercury arc lamp or a globar as source [11]. Evidently spectrometers with sources of high output power and small linewidth, i.e., with high spectral brightness, offer the best sensitivity if MHz resolution is required. Essentially this is caused by the high spectral brightness of the source in combination with excellent sensitivity of the cryogenic detectors. In a similar way to QCLs, the p-type Ge laser can emit THz radiation [12] with typically a lower average power on the order of 0.1 mW, while high peak power above 40 W [13] covering a broad spectral range with a single device is obtainable [12], [14].

Using room-temperature detectors decreases the sensitivity by several orders of magnitude. The photomixer spectrometer is less sensitive than other cw spectrometers as its spectral brightness is quite low. For a spectral resolution of 3 GHz a TDS has a similar performance to cw spectrometers. However, when scaling to 1 MHz resolution the performance deteriorates drastically, because the high sensitivity of its detection scheme cannot compensate for the low spectral brightness of the source. Similarly, the sensitivity of FTS is lower because of the low source power. FTS can be comparable or superior to TDS depending on the detector and the frequency used. For the parameters chosen here the cross-over occurs at about 2 THz. Using a Golay cell or pyroelectric detector with a two to three orders of magnitude larger NEP will move this cross-over to about 3 THz. This cross-over has also been found in another study which compared the performance of TDS and FTS [9]. The comparable performance of the FTS is due to the cw mode in which it is operated, while TDS has a very low duty cycle and low average power. When measuring broader absorption features the situation changes to some extent. For example if a 30 GHz wide absorption feature is to be measured the power of an FTS or TDS is approximately 10 times larger than in 3 GHz bandwidth which is considered in Fig. 1. Accordingly the minimum detectable absorption will be 10 times smaller. We note that TDS has advantages in comparison to FTS providing absorption measurements as a function of time with ps to sub-ps time resolution and easy access to phase information and, therefore, the refractive index of a sample. We limit here our discussion on those applications where absorption of a sample as a function of frequency is of key interest.

In real spectrometers the minimum detectable absorption is usually larger than the calculated one because other effects, such as power fluctuations of the source or standing waves in the spectrometer, are the most severe limitation. Some of these effects are discussed in the following sections. It should be noted that the sensitivity of a spectrometer can be increased significantly when using a source with higher output power. Alternatively the lack of source power can be compensated by using a more sensitive detector.

III. Spectroscopy With CW Quantum Cascade Lasers

Fig. 1 indicates how powerful a spectrometer with a QCL as the radiation source can be. In terms of sensitivity it outperforms alternative spectrometers in the same frequency range covered by QCL sources. High resolution molecular spectroscopy with a THz QCL was demonstrated for the first time with a distributed feedback device. The absorption of a rotational transition of methanol at 2.519 THz, as well as the pressure broadening and the pressure shift of this transition, were measured [15]. In this spectrometer the absolute frequency was determined by mixing the radiation from the QCL with that from an optically excited THz gas laser. Amplitude as well as frequency modulation schemes were applied. As a first application the emission of a QCL was locked to a molecular transition with sub-MHz accuracy [16]. This is required, for example if the QCL is used as local oscillator in a heterodyne spectrometer [17]. Using a QCL with a Fabry-Pérot resonator instead of a DFB laser leads to a much more complicated spectrum because the modes are emitted simultaneously and each mode generates a particular spectrum. When tuning the current of the QCL, and thereby the frequency, all modes of the QCL generate spectra simultaneously. The combination of these is difficult to interpret without any *a priori* knowledge of the expected spectrum [18], [19]. In this section we will discuss recent progress toward a THz spectrometer based on a QCL. Three aspects are discussed: sensitivity, frequency calibration, and frequency multiplexing.

The QCL used in these experiments was developed at the Paul-Drude Institut für Festkörperelektronik in Berlin. The active region is based on a two-miniband design, in which efficient injection into the upper laser level is achieved by an intersubband transition resonant to the energy of the longitudinal

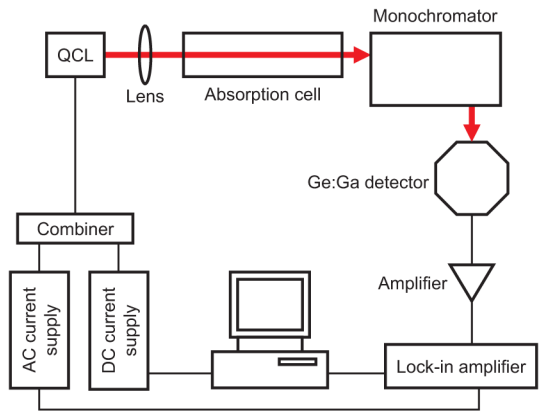

Fig. 2. Setup of the THz spectrometer with QCL.

optical phonon [20]. The laser has a single-plasmon waveguide and a Fabry-Pérot cavity with both facets uncoated. The laser ridge is 10 μm high, 100 μm wide, and 1.2 mm long. The electrical contacts are wire-bonded to the top layer and to both sides of the laser ridge. The chip with the QCL was soldered with indium onto a gold-plated copper submount and attached to a second copper mount. This in turn is fixed to the cold finger of a compact air-cooled cryocooler (model K535 from Ricor). Cold finger, copper mounts, and the QCL are encapsulated in a vacuum housing. Prior to operation, the housing is evacuated to a pressure of less than 1 Pa. The output window is made from z-cut quartz. In order to avoid standing waves and to minimize Fabry-Pérot type etalon effects in the setup and back reflections into the laser, the output window is tilted with respect to the optical axis. The current for the QCL was supplied by a home-made, battery-driven current source. A more detailed description of the QCL and the system in the cryocooler is given in [19]. The emission spectrum of the QCL has several modes with a spacing of 31 GHz. The output power of the laser is 4 mW at a current of 600 mA and a temperature of 45 K.

The setup of the spectrometer is shown in Fig. 2. The beam emitted by the QCL is focused with a TPX lens onto the entrance slit of a monochromator (model Acton SP2300). A 27-cm long glass absorption cell was placed between the lens and the monochromator. The 1-mm thick high-density polyethylene windows of the cell were tilted in order to minimize standing waves. The pressure in the cell was measured by a capacitive manometer. A Ge:Ga detector followed by a low-noise amplifier was placed at the output of the monochromator. Frequency tuning of the spectrometer was achieved by two methods. Coarse frequency tuning was achieved by tuning the monochromator to one particular mode of the QCL. Fine tuning of the frequency was accomplished by changing its current or the heat sink temperature. By this means a tuning range of approximately 10 GHz was obtained for each of the laser modes. The current of the QCL was modulated at a frequency of 10 kHz with a peak-to-peak amplitude of 1.7 mA by superposition of the modulation current from a frequency synthesizer with a DC current. The output signal from the low-noise amplifier was detected with a lock-in amplifier using the 10 kHz current modulation as a reference. Control of the laser current as well as data acquisition is carried out by a computer and a dedicated LabVIEW© control software which acquires the direct transmission signal, and the first (1f) and the second harmonic (2f) signal from the lock-in amplifier simultaneously. An example of a spectrum of CH_3OH at a pressure of 1 hPa is shown in Fig. 3. The 4.5 GHz wide portion of the spectrum was measured by tuning the laser current in steps of 0.25 mA which corresponds to frequency steps of 5 MHz. The integration time for each spectral resolution element was 40 μs, resulting in a total integration time of only 36 ms for the whole spectrum. Frequency calibration was obtained by comparison with the same CH_3OH spectrum measured with an FTS. The direct transmission spectrum suffers from the change of output power with current, which leads to a strong baseline variation and two steps in the output power that are probably caused by electric-field domains in the active medium of the laser [20]. This is eliminated to a large extent in the 1f spectrum while in the 2f spectrum it disappeared completely. The peak power of this particular laser mode is approximately 1.5 mW. Of this about 30% is absorbed in the optical path through the atmosphere and 30% are losses by the windows of the absorption cell and the detector cryostat. In addition the transmission of the monochromator is approximately 30%. This leads to a power of 220 μW on the Ge:Ga detector in good agreement with 180 μW measured with a Golay cell detector at the output of the monochromator.

The sensitivity of the spectrometer can be determined by measuring an absorption line using amplitude modulation. This allows measurement of the absolute absorption directly. With a 1 s integration time for each spectral resolution element the (S/N)-ratio of 20 to 100 for the absorption features in Fig. 3 corresponds to a fractional absorption of approximately 10^{-5}. This is about three orders of magnitude more than expected for the minimum detectable absorption as calculated from (1). In the present setup the (S/N)-ratio is limited by standing waves between the detector and the QCL which induce baseline fluctuations. Eliminating the standing waves will improve the minimum detectable absorption by up to two orders of magnitude. The performance of the spectrometer might be compared with that of a tunable THz spectrometer based on frequency mixing of radiation from an optically pumped gas laser with that from a frequency-tunable microwave source. The minimum detectable absorption of this spectrometer is 10^{-5} to 10^{-6} [7]. Yet another comparison is a spectrometer that was equipped with a 2-m long absorption cell and a multiplier-based THz source. With this a fractional absorption of 10^{-3} was demonstrated for a rotational transition of N_2O at 1.09 THz. In that case, the sweep time was 1 s for 20 spectral resolution elements and the observed (S/N)-ratio was 30 [5].

As pointed out in the introduction the total time needed for data acquisition is what counts in many applications. In order to increase the measurement speed and frequency coverage of a QCL-based spectrometer all modes emitted by the QCL should be detected simultaneously. This leads to a frequency multiplexing scheme as known from grating spectroscopy in the visible part of the electromagnetic spectrum, where the exit slit of the grating spectrometer is replaced by a linear CCD detector. An additional advantage is that such a spectrometer has

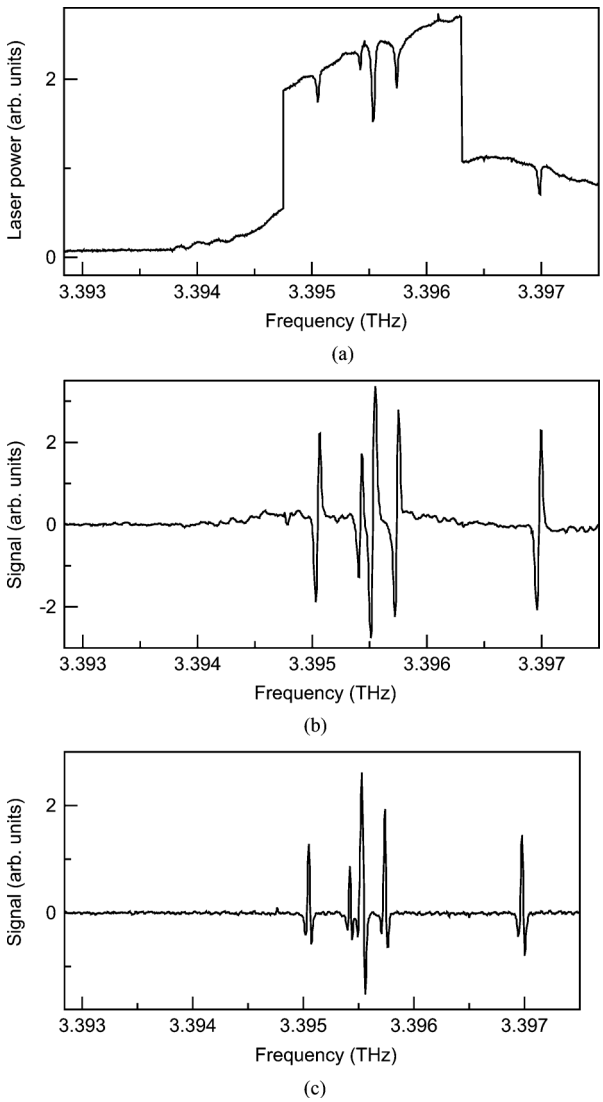

Fig. 3. Spectrum of CH_3OH. (a) measured in direct transmission, (b) measured with 1f lock-in detection, (c) measured with 2f lock-in detection.

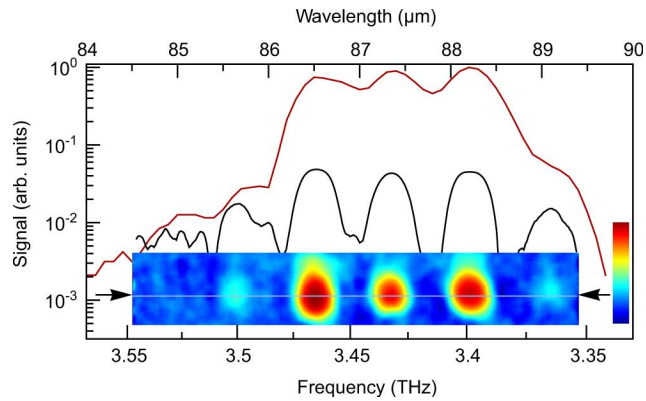

Fig. 4. Emission modes of a 3.4-THz QCL with Fabry-Pérot resonator measured with a grating monochromator and a Golay cell detector (upper red line) and imaged with a microbolometer camera (inset with color scale) shown both in logarithmic scale. A line trace (lower black line) of the image data is also displayed taken at the image line position marked by the arrows. The exit slit was removed at the output of the monochromator. Three strong and several weak modes, one on each side of the three strong ones, are visible. Five modes are detectable with the Golay cell as well as with the microbolometer camera.

no moving parts and fast electrical frequency tuning can be implemented. To demonstrate the feasibility of this approach a similar setup, as shown in Fig. 2, is used. The main difference is that the Ge:Ga detector is replaced by an IR camera (model VarioCAM from InfraTec G.m.b.H. [21]). The core of the camera is a microbolometer array with 640×480 pixels. The size of the array is 16×12 mm^2 and the pixel pitch is 25 μm. Each microbolometer is made from amorphous silicon. In order to use the camera at THz frequencies the Ge lens was removed so that the THz radiation impinges directly on the array. The exit slit of the monochromator was also removed. The resulting exit opening was 17 mm. This enabled the simultaneous imaging of five laser modes without any additional optical element between the monochromator and the array (Fig. 4). With an optimized monochromator, and dedicated optics which image the output of the monochromator onto the array, it seems feasible to monitor up to approximately 20 emission modes of a QCL simultaneously by frequency multiplexing. Assuming a frequency tunability of 5 to 10 GHz per mode by varying the current through the QCL an instantaneous frequency coverage in the order of 100 GHz is feasible. This is still much less bandwidth than a TDS or FTS offer, but sufficient for many applications.

IV. Spectroscopy With Ge Detectors and Pulsed Ge THz Lasers

Pulsed THz sources are frequently employed for spectroscopy. One example is the Ge THz laser spectrometer. Although the high electrical power consumption limits the cooling of Ge THz lasers, resulting in an average power of about 0.1 mW, it is possible to generate very high peak pulse power of up to 1 W and beyond, for example 40 W with larger crystals [13]. Combining a p-type Ge:Be laser with a Ge:Al photoconductor [22] and a blazed grating with a grating constant of 0.1 mm results in a very sensitive spectrometer [23]. This spectrometer allows the investigation of strongly absorbing substances such as polar liquids, for example water, in the THz range [24] as well as aqueous protein solutions [25], [26]. The spectrometer benefits from the very high sensitivity of liquid helium cooled, unstressed Ge photodetectors with background limited performance (NEP close to $10^{-14}\mathrm{W}/\sqrt{\mathrm{Hz}}$) in the spectral range from 2.1 THz to several THz. The NEP of such photodetectors is even three orders of magnitude lower if low photon flux and low background conditions are used. As outlined in [7] the detector should be able to achieve shot noise limited performance. For a typical bandwidth of 100 MHz to record individual 4 μs Ge laser pulses the NEP is close to 10^{-10} W resulting in a large dynamic range. The intrinsic line width of the laser is Fourier limited, due to the pulse length employed and is less than 1 MHz [23]. With external tunable resonators, and by changing an external magnetic field, it is possible to tune the emission frequency in a single longitudinal mode [23], [27], [28] from about 1 THz to beyond 4 THz [14]. In the current setup the laser is mounted in a closed-cycle cryocooler (Sumitomo Heavy Industries) with 1 W cooling power at 4.2 K and operated with a commercial pulse generator (Avtech Electrosystems Ltd.). The Ge:Be laser is used without an external resonator which leads to broad band emission

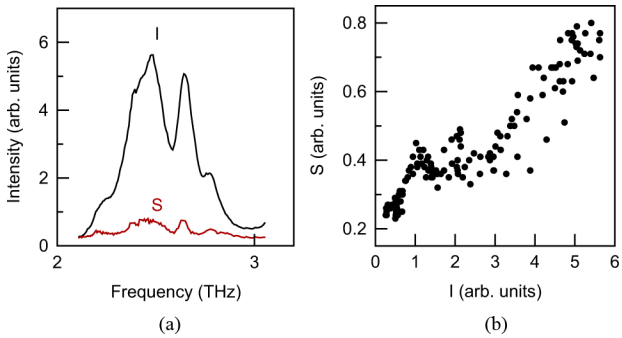

Fig. 5. (a) Measured Ge:Be laser THz intensity I as a function of frequency using a grating spectrometer and a Ge:Al photodetector while in air visible by the presence of water vapor absorption and standard deviation S of single measurements using only two pulses for evaluation per frequency bin (i.e., integration time of $8\ \mu$s per bin) of the grating. The standard deviation from the average which gets smaller by the square root of the number of pulses collected is not shown. (b) Standard deviation S of single measurements as a function of intensity indicating a roughly 10% correlation for an $8\ \mu$s integration time.

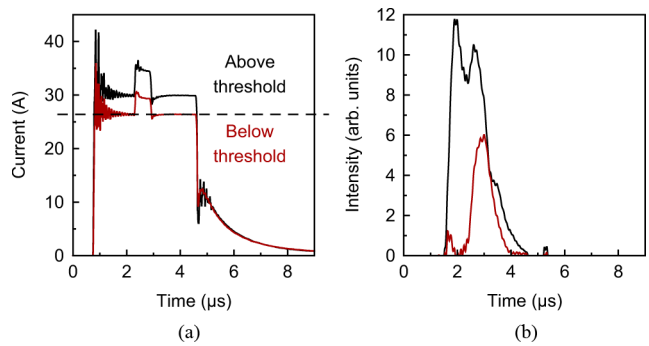

Fig. 6. (a) Current traces of a Ge:Be laser operated just below and above threshold with additional current pulse applied in the time from 2.5 to 3 μs. (b) Laser signals detected with a Ge:Al photodetector (detector response time of approximately $0.3\ \mu$s leading to a slow increase and exponential decay after the laser emission due to current excitation stops).

consisting of several thousand narrow modes spanning a frequency range of 1 THz (Fig. 5). The broad spectral range is partially a result of the permanent magnets employed, which lead to a field inhomogeniety across the 360 mm^3 crystal so that different parts of the crystal support different frequencies. The Ge:Al detector allows detection above 2.1 THz and is most sensitive around 2.7 THz due to the ionization energy of the Al acceptors.

A. Intensity and Gain Modulation

Ge lasers in crossed electric and magnetic fields at low, cryogenic temperature can emit very short, theoretically ps long, pulses by using modelocking schemes with a radiofrequency synchronized to the round-trip time of the laser pulse within the laser cavity, and applied to two additional electrical contacts on the Ge crystal [29], [30], [31]. Pulses of a few tens of ps have been demonstrated [30]. However, it is also possible to modulate the laser current directly to generate short pulses while modulating close to the laser threshold. In pulsed operation the main difficulty in achieving very short pulses is the impedance mismatch between the pulse generator and a cryogenically cooled laser. At cryogenic temperature, before the electric pulse excitation, the resistance for a semiconductor laser is typically high (for low doped Ge several kOhm) while it is moderate (10 to 20 Ohm) during the pulse. A scheme to operate the laser just below threshold, while modulating the current during the pulse, could be a solution especially if the laser can be tuned over a wide range of currents and voltages for operation at various output frequencies.

Fig. 6 shows a proof-of-principle experiment in which a current pulse for operating the Ge laser just below and above the laser threshold is applied. Ringing is visible, due to the impedance mismatch between the cold and the current-driven conditions. Although the pulse generator was not optimized to match the impedance for the operating current it is evident that, if a current is already flowing, the change in impedance is small if an additional short pulse is applied. In consequence, only a little ringing and fast switching of the gain is observed. Even above threshold an additional pulse can increase the intensity of the THz pulse due to higher gain at higher fields for the magnetic induction used. Resolving the pulse length and sharpness of the transition was limited due to the $0.3\ \mu$s response time of the photoconductor. The possibility of modulating the current even in a short time interval of a few μs can allow the implementation of current modulation schemes even for larger crystals and subsequently high power Ge THz lasers.

B. Standard Deviation of Germanium Laser Pulse Intensity

While controlled fluctuations are beneficial for short pulse generation or current modulation techniques we find that THz laser pulses fluctuate with an intensity which scales with the emission power (Fig. 5(b)). The standard deviation of a single measurement S is about 10% using single $4\ \mu$s long pulses which correspond to the integration time. For repeated measurements and increasing integration and measurement time the standard deviation of the mean value reduces with the root integration time or number of pulses averaged, respectively, which can be very low. The laser system leads to a very small statistical error in the absolute absorption coefficient (for example for water with $400 - 500$ cm^{-1}) of less than 0.1% corresponding to 0.3 cm^{-1} for 3000 pulses each $5\ \mu$s long corresponding to 15 ms total integration time. For such low statistical errors systematic errors become dominant. The systematic errors are not related to the Ge laser spectrometer itself but are caused by the heterogeniety of the liquid sample outlined in the next section.

Fig. 7(a) shows the distribution of pulse traces for several thousand pulses corresponding to a total integration time of 10 ms, and two traces reflecting the development of the mean intensity value of pulses alternating between two arms of a difference spectrometer [26]. The pulses are directed by a metalized chopper blade either into the sample arm or into the reference arm within a few ms. The switching speed is limited by the mechanical stability of the chopper motor and blades to 60 to 100 Hz and not by the Ge laser which could be pulsed at a higher frequency. Measuring the difference between the two pulses reduces systematic errors due to any small amount of water vapor

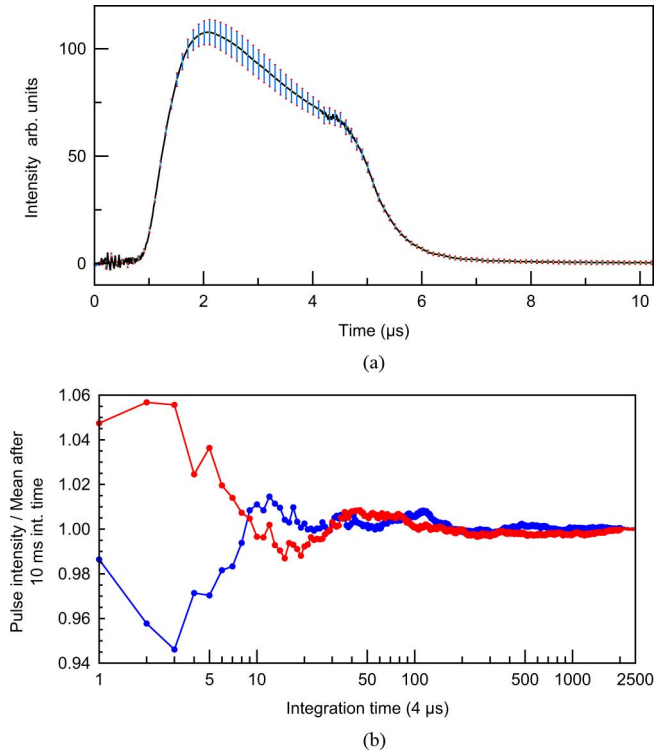

Fig. 7. (a) Standard deviation of individual 2500 Ge laser pulses, i.e., 10 ms total integration time, around the mean pulse shape. The standard deviation of the mean is 50 times smaller and not visible in this scale. (b) Intensity fluctuations in two arms of a two beam difference spectrometer normalized to the average value after 10 ms integration time, i.e., 2500 pulses.

remaining in the sample and reference chamber, as well as fluctuations due to the sample and reference temperature control thermostat which was stable within ± 0.01 K.

C. Systematic Errors Due to a Sample

It is important to note that pulse to pulse instabilities observed from all pulsed sources, due to small fluctuations interdependently connected to temperature variations of a heat sink (in cryogenic systems but also in room temperature devices), impedance mismatch of power supplies to the active gain medium, and current fluctuations, are all contributing to increase the value of the minimum detectable absorption. These source contribution can dominate the overall performance while the detector noise of cryogenically cooled direct detectors is often so low that these are only limited by unavoidable background radiation of the 300 K environment.

At THz frequencies systematic errors can occur which are due to the sample itself and not the spectrometer. Often these dominate the error obtained in a single measurement even if a longer integration time is used. These systematic errors might be due to the consistency of the sample itself. For example, in aqueous solutions with proteins, foaming, bubble formation, impurity inclusion, and sedimentation can occur. It is therefore necessary to minimize the total measurement time but retain high (S/N)-ratios. These systematic errors can be evaluated and reduced by measuring several, very similarly prepared samples in fast switching difference spectrometers. For example, the error is much smaller if a pure liquid reference with comparable absorption and with the same thickness is used to determine the ratio of sample/reference and not an empty sample cell as reference. The errors due to standing waves and interference at interfaces, for example between window and solution, are minimized.

Exchanging the sample and reference and placement of the holder can also affect the signal because the Gaussian beam propagation depends exponentially on small beam tilts and off-axis shifts [32]. The reproducible placement of the sample holder and, at the same time, allowing a sufficient sampling of random orientations in tilt and position around the optimum sample position is required to achieve reliable data. As an example it was found, that for a peptide solution in water [26], [33] it was not possible to obtain unambiguously a non-linear relation between peptide concentration and THz absorption coefficient within the error bars using an FTS with a liquid helium cooled bolometer. The reason was the low (S/N)-ratio in the same measuring time (not integration time) although the FTS benefits from cw radiation. The measurement time for 30000 pulses with the Ge laser difference spectrometer for each channel (sample and reference) and the set chopper speed was approximately 7.5 minutes. With exchange, cleaning, new filling and thermal equilibrium of the solution a measurement time of 20 to 30 minutes is needed for each measurement which was also used for the total scanning time in each FTS measurement [26]. The systematic errors are especially evident for high peptide concentrations in FTS but not in the Ge laser spectrometer. We obtain an error in the absorption coefficient of ± 0.3 cm^{-1} in comparison to ± 20 cm^{-1} for FTS. This is due to the very viscous solution for increasing concentration which lead to larger errors for FTS which detects close to the noise level for such strongly absorbing liquids.

V. Random Error in Intensity Spectra Observed With THz Time-Domain Spectroscopy

In THz TDS based on an Auston switch fast electromagnetic pulses are generated and detected by optical pulses [34]. This technology has progressed rapidly with the development of femtosecond (fs) lasers (see for example [35]). THz pulses are generated in an emitter such as a photoconductive antenna (PCA) or a nonlinear optical crystal and they are detected in a THz detector. The latter is usually a similar device as the emitter. The THz electric field waveform is traced out by changing the optical path length between THz pulses and the probing fs laser pulses by using a moving optical-delay stage [36], or by using two fs lasers in an asynchronous optical sampling arrangement [37].

At present THz TDS is one of the most widespread, room temperature technologies for spectroscopic applications, but the accuracy in measurements is often not evaluated systematically. The systematic study of errors requires long term measurement over several hours, and an extra effort to evaluate all parameters of a spectrometer.

We have studied the random errors in intensity and phase spectra by taking a number of THz TD spectra repeatedly. Several characteristic properties of standard deviation random errors in intensity and phase spectra appear. The standard deviation discussed in this section is an experimental standard de-

viation defined as the square root of variance which is devided by a number of observations minus one. The standard deviation σ_I in the intensity spectrum I was relatively large $\sigma_I/I \approx 0.01$ [38] whereas σ_Φ in the phase spectrum Φ was rather small $\sigma_\Phi/\Phi \approx 3\times10^{-4}$ [39]. The former means that the (S/N)-ratio, calculated from the intensity divided by its standard deviation, is much smaller than the dynamic range $(10^5 \text{ to } 10^7)$ defined by the ratio of the maximum in the intensity spectrum to the noise floor which is about equal to the noise level without THz irradiation [40], [41]. The noise floor mainly results from noise sources in the receiver as discussed by van Exter and Grischkowsky [42]. Nevertheless, the large dynamic range is the prime advantage of THz TDS because it is related to the maximum absorption coefficient which can be measured, but the (S/N)-ratio which directly determines the minimum detectable absorption is also important. Naftaly and Dudley have also demonstrated almost the same (S/N)-ratio in the intensity spectra in comparison to our observation in their THz TDS measurements [43]. Therefore, we conclude that the evaluation of standard deviations in the intensity spectra is necessary for almost all applications of THz TDS because they significantly affect the accuracy during observations. A further goal of this study is to determine the instrument function of a THz TDS spectrometer which consists of a number of different components. With the knowledge of an instrument function the total measurement time could be reduced significantly and reliable data including error estimates for samples are predictable even with lower priced components and short total measurement time. In the following we discuss in more detail the random errors in the intensity spectra for a specific THz TDS system detailed below. Although these errors might significantly vary in value between different THz TDS, for example, due to different fs lasers with high or low power, the use of stabilized power supplies for pump lasers, fiber coupling schemes or fiber lasers, and investigated THz frequency range, it is still possible to identify common origins of errors in THz TDS.

A. Measurement of Standard Deviations in the Intensity Spectra

A transmission-type THz TDS device (Tochigi Nikon Corp.) with low-temperature-grown GaAs photoconductive antennas (LT-GaAs PCAs) as a THz-emitter and a detector is used for the study of the random error in THz TDS measurements. An fs fiber laser of IMRA Inc. (Femtolight) with an average power of 20 mW and a pulse repetition frequency of 50 MHz then excites the THz emitter and probes the detector. Using this spectrometer, THz pulse waveforms are sampled by 1024 data-points in 12 μm intervals of optical delay, for which the frequency resolution of the measurement is 0.024 THz, the integration time of one data-point is 240 ms, and one scan requires about 10 min of measurement time. The waveforms measured without a sample (hereafter referred as "reference") are shown in Fig. 8(a). Scans to measure reference and a sample are repeated 16 times, respectively, for a statistical analysis and to calculate mean and standard deviation. Fig. 8(b) displays the drifts in both amplitude and time-position of the pulse maximum in the THz waveform during a measurement time of about 6 hours. The maximum amplitudes of the THz waveforms are plotted as a function of the starting time of each scan for 16 scans in Fig. 8(c), displaying the THz amplitude drift. The magnitude of the drifts in amplitude and time-position depend on the specific instrument used, but the drifts exist more or less in all instruments. Usually the optical parameters of a sample are derived from a calculation of sample/reference for which the data are taken closely in time, and hence such drifts do not affect much the resultant values. Because the drift is not due to a random error, we can correct it by fitting a function to the change in amplitude in order to investigate only the remaining characteristics of random error. The drift in the reference measurement was correlated with that of the samples, when the reference (R) and sample (S) are measured in a sequence like $R_0,\ S_0,\ S_1,\ R_1,\ R_2,\ S_2, \ldots, S_{m-1},\ S_m$, and R_m, where subscript m is an integer (m is 16 in this case). The chosen method to measure alternately reference and sample is useful to correct the drift in the sample measurement by the reference measurement.

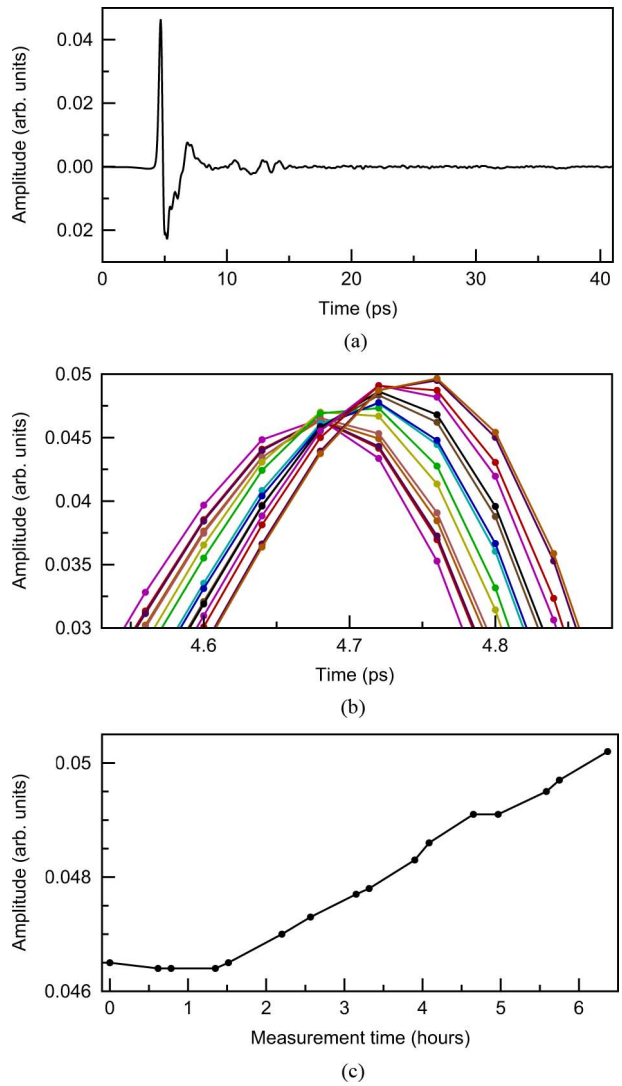

Fig. 8. (a) THz pulse waveform measured with a THz TDS using LT-GaAs PCAs as an emitter and a detector described in detail in the text. (b) Change in amplitude and time position of the peak maximum of 16 THz pulse waveforms for the described TDS. (c) Drift in amplitude of the peak maximum of 16 THz pulse waveforms over a long measurement time of 6 hours.

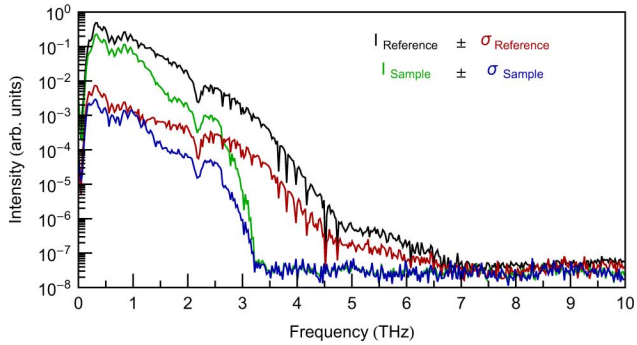

Fig. 9. Mean and standard deviation of intensity spectra calculated from 16 measurements by the THz-TDS with the LT-GaAs PCA detector.

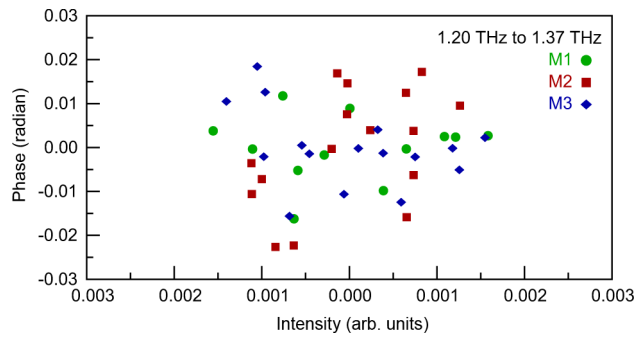

Fig. 10. Deviations from the mean in the intensity and phase spectra at 1.20 to 1.37 THz plotted on the phase-intensity diagram; displaying the correlation of random errors between phase and intensity for 3 measurements.

B. Characteristics and Origin of Standard Deviations in the Intensity Spectra

The mean intensity spectra and standard deviations of reference and sample are calculated after the drift correction and shown in Fig. 9. The sample is a ZnTe crystal 1.496 mm thick produced by Nippon Mining and Metals Co. Ltd. The standard deviation in intensity is correlated with the corresponding intensity spectrum and the ratios σ_I/I of standard deviation σ_I to intensity I are about 0.01 for both in the frequency regions of high intensity as displayed in Fig. 9. That both, the reference and the sample, show almost the same characteristic σ_I/I can be understood by the assumption that the amplitude of the THz pulse signal fluctuates naturally because I and σ_I decrease in the same manner by the absorption and reflection of a sample.

The open question is whether a correlation exists in random errors between intensity and phase. Deviations from the mean in 44 intensity and phase spectra of the reference, taken in three different long term measurements at a frequency of 1.20 to 1.37 THz, are plotted in an intensity-phase diagram shown in Fig. 10. The points are randomly scattered, meaning that there is almost no correlation between intensity and phase. This result is confirmed at other frequencies in the range of 0.34 to 0.51 THz, 1.44 to 1.61 THz, 1.76 to 1.93 THz, and 2.44 to 2.61 THz. Therefore, we assume that the origin of the random error in the intensity spectrum is different from that of the phase error.

The origin of the intensity fluctuation has been investigated in detail in [44] with the exception of the beam deflection fluctuations of the fs laser. Power fluctuations of the fs laser expressed as the ratio of standard deviation to the mean laser power for the same duration as the THz measurement were 6.2×10^{-4}, which were more than one order of magnitude smaller than that of the THz intensity. Timing jitter of the fs-laser pulse source itself and due to path length variations between detection and emission path could contribute as well but is mostly cancelled out in the configuration of the THz TDS in which each pulse of the fs laser is used for both, emission and detection of the THz pulse. Staggering the optical delay line and change in atmospheric THz absorption during measurements did not affect the THz intensity variation in our measurements due to the compact design and dry air/nitrogen used.

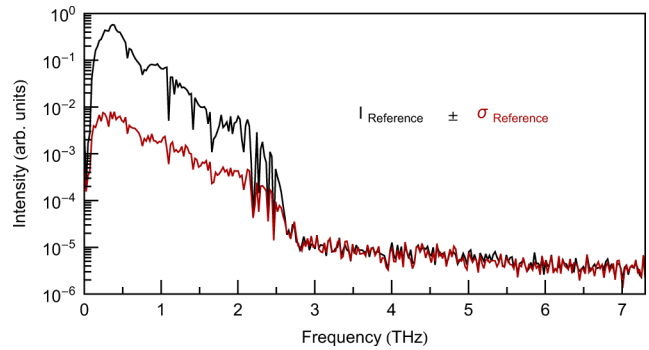

Fig. 11. Mean and standard deviation of intensity spectra calculated from 16 measurements by replacing the LT-GaAs PCA detector in the THz-TDS with a ZnTe EO detector.

Another THz TDS system which adopts a ZnTe-EO crystal 1.5 mm thick instead of a LT-GaAs PCA as a THz detector was used to determine the random error of the THz intensity. The other conditions of the measurement were almost the same as described before. The intensity spectra I and standard deviations σ_I measured by the ZnTe-EO detector are shown in Fig. 11. Again the ratio σ_I to I is about 0.01 in the frequency regions of high intensity. The σ_I/I is very similar in both measurements although, using two different THz detectors, we find that the THz detector is not the main origin of the random error in the THz intensity.

A possible origin of the intensity error is beam deflection fluctuations of the fs laser. The change of beam position at the distance of the THz emitter was observed, together with amplitude changes in the THz pulse amplitude. The experimental result shows that the standard deviation in the beam deflection of the fs laser was about a few μm at the THz emitter position, which is smaller than the gap of 6 μm and the width of 10 μm of the LT-GaAs PCA (Hamamatsu Photonics K. K., G10620–03). The beam deflection of the fs laser could be a cause of the random error in the THz intensity for which further investigations are under way to quantify the relation between beam deflection and change of THz amplitude.

Random error in the intensity spectrum measured with THz TDS, which is about 1% of the intensity in the frequency ranges of high THz intensity, needs to be carefully considered in all measurements using THz TDS, because it is much larger than the ratio of the noise floor level to the maximum intensity, which is the inverse of the dynamic range and lies typically between 10^{-5} to 10^{-7}.

VI. Summary and Conclusion

In this article we have presented system and sensitivity considerations, which have allowed us to evaluate THz spectrometers and to provide some guidelines to choose the appropriate source-detector combination for a given sample under study. The systematic investigation and comparison of different THz spectrometers is an attempt to identify common limitations and sources of errors in THz measurements. Single frequency, as well as frequency multiplexing, for example by QCL and array based grating spectroscopy, gain modulation in Ge lasers to achieve very short pulses for high time resolution, or broad band pulses with high spectral resolution in THz TDS, are illustrating the potential wide range of technical solutions in the THz frequency range.

Acknowledgment

All authors contributed equally to this work. One of the authors, H.-W. Hübers, thanks his colleagues from DLR and Paul-Drude-Institut für Festkörperforschung for their support. N. Hiromoto would like to express his thanks to Drs. K. Sakai and I. Hosako of NICT, Mr. T. Hirosumi and Dr. H. Ohtake of AISIN SEIKI Co. Ltd. for their support and advice. The work by N. Hiromoto and E. Bründermann is supported by the FRIRUN agreement. E. Bründermann would like to thank E. E. Haller for support on Ge lasers and photodetectors and S. Funkner for contributions to systematic studies of the Ge laser spectrometer and samples. The authors also thank the reviewers for valuable suggestions to improve the article.

References

[1] F. C. De Lucia, "Sensing with terahertz radiation," in *Spectroscopy in the Terahertz Spectral Region*. New York: Springer, 2002.

[2] E. Bründermann, H.-W. Hübers, and M. F. Kimmitt, *Terahertz Techniques*. New-York: Springer, 2011.

[3] A. A. Volkov, Y. G. Goncharov, G. V. Kozlov, S. P. Lebedev, and A. M. Prokhorov, "Dielectric measurements in the submillimeter wavelength region," *Infr. Phys.*, vol. 25, no. 1/2, pp. 369–373, 1985.

[4] G. Kozlov and A. Volkov, "Millimeter and submillimeter wave spectroscopy of solids," in *Coherent Source Submillimeter Wave Spectroscopy*. New York: Springer-Verlag, 1998, pp. 51–109.

[5] B. J. Drouin, F. W. Maiwald, and J. C. Pearson, "Application of cascaded frequency multiplication to molecular spectroscopy," *Rev. Sci. Instr.*, vol. 76, pp. 093-113-1–093-113-10, 2005.

[6] S. Matsuura, M. Tani, and K. Sakai, "Generation of coherent terahertz radiation by photomixing in dipole photoconductive antennas," *Appl. Phys. Lett.*, vol. 70, no. 5, pp. 559–561, 1997.

[7] G. A. Blake, K. B. Laughlin, R. C. Cohen, K. L. Busarow, D.-H. Gwo, C. A. Schmuttenmaer, D. W. Steyert, and R. Saykally, "The Berkeley tunable far infrared spectrometers," *Rev. Sci. Instrum.*, vol. 62, pp. 1701–1716, 1991.

[8] Y. Kim, D.-S. Yee, M. Yi, and J. Ahn, "High-speed high-resolution terahertz spectrometers," *J. Kor. Phys. Soc.*, vol. 56, no. 1, pp. 255–261, 2010.

[9] P. Y. Han, M. Tani, M. Usami, S. Kono, R. Kersting, and X.-C. Zhang, "A direct comparison between terahertz time-domain spectroscopy and far-infrared Fourier transform spectroscopy," *J. Appl. Phys.*, vol. 89, no. 4, pp. 2357–2359, 2001.

[10] B. Williams, "Terahertz quantum cascade lasers," *Nature Photon.*, vol. 1, pp. 517–525, 2007.

[11] M. Abo-Bakr, J. Feikes, K. Holldack, G. Wüstefeld, and H.-W. Hübers, "Steady-state far-infrared coherent synchrotron radiation detected at BESSY II," *Phys. Rev. Lett.*, vol. 88, pp. 254-801-1–254-801-4, 2002.

[12] E. Bründermann, "Widely Tunable Far Infrared Hot Hole Semiconductor Lasers," in *Long-Wavelength Infrared Semiconductor Lasers*. New York: Wiley, 2004, pp. 279–350.

[13] A. V. Muravjov, H. Saxena, R. E. Peale, C. J. Fredricksen, O. Edwards, and V. N. Shastin, "Injection-seeded internal-reflection-mode p-Ge laser exceeds 10 W peak terahertz power," *J. Appl. Phys.*, vol. 103, p. 083112, 2008.

[14] L. A. Reichertz, O. D. Dubon, G. Sirmain, E. Bründermann, W. L. Hansen, D. R. Chamberlin, A. M. Linhart, H. P. Röser, and E. E. Haller, "Stimulated far-infrared emission from combined cyclotron resonances in germanium," *Phys. Rev. B*, vol. 56, no. 19, pp. 12 069–12 072, Nov. 1997.

[15] H.-W. Hübers, S. G. Pavlov, H. Richter, A. D. Semenov, L. Mahler, A. Tredicucci, H. E. Beere, and D. A. Ritchie, "High resolution gas phase spectroscopy with a distributed feedback terahertz quantum cascade laser," *Appl. Phys. Lett.*, vol. 89, p. 061115, 2006.

[16] H. Richter, S. G. Pavlov, A. D. Semenov, L. Mahler, A. Tredicucci, H. E. Beere, D. A. Ritchie, and H.-W. Hübers, "Sub-megahertz frequency stabilization of a terahertz quantum cascade laser to a molecular absorption line," *Appl. Phys. Lett.*, vol. 96, p. 071112, 2010.

[17] H.-W. Hübers, "Terahertz heterodyne receivers," *IEEE Sel. Topics Quantum Electron.*, vol. 14, no. 3, pp. 378–391, Mar./Apr. 2008.

[18] H.-W. Hübers, S. G. Pavlov, H. Richter, A. D. Semenov, L. Mahler, A. Tredicucci, H. E. Beere, and D. A. Ritchie, "Molecular spectroscopy with terahertz quantum cascade lasers," *J. Nanoelectron. Optoelectron.*, vol. 2, pp. 101–107, 2007.

[19] H. Richter, M. Greiner-Bär, S. G. Pavlov, A. D. Semenov, M. Wienold, L. Schrottke, M. Giehler, R. Hey, H. T. Grahn, and H.-W. Hübers, "A compact, continuous-wave terahertz source based on a quantum-cascade laser and a miniature cryocooler," *Opt. Exp.*, vol. 18, pp. 10 177–10 187, 2010.

[20] M. Wienold, L. Schrottke, M. Giehler, R. Hey, W. Anders, and H. T. Grahn, "Low-voltage terahertz quantum-cascade lasers based on LO phonon-assisted interminiband transitions," *Electron. Lett.*, vol. 45, pp. 1030–1031, 2009.

[21] E. Bründermann, J. Ränsch, M. Krauss, and J. Kunsch, "Erste THz-Videos mit einer Silizium-basierten IR-Kamera," *Photonik*, vol. 6, pp. 60–63, 2006.

[22] E. Bründermann, A. M. Linhart, L. Reichertz, H. P. Röser, O. D. Dubon, W. L. Hansen, G. Sirmain, and E. E. Haller, "Double acceptor doped Ge: A new medium for inter-valence-band lasers," *Appl. Phys. Lett.*, vol. 68, no. 22, pp. 3075–3077, May 1996.

[23] E. Bründermann, H. P. Röser, A. V. Muravjov, S. G. Pavlov, and V. N. Shastin, "Mode fine structure of the FIR p-Ge intervalenceband laser measured by heterodyne mixing spectroscopy with an optically pumped ring gas laser," *Infrared Phys. Technol.*, vol. 36, no. 1, pp. 59–69, 1995.

[24] A. Bergner, U. Heugen, E. Bründermann, G. Schwaab, M. Havenith, D. R. Chamberlin, and E. E. Haller, "New p-Ge THz laser spectrometer for the study of solutions: THz absorption spectroscopy of water," *Rev. Sci. Instr.*, vol. 76, pp. 063 110/1–063 110/5, 2005.

[25] S. Ebbinghaus, S. J. Kim, M. Heyden, X. Yu, U. Heugen, M. Gruebele, D. M. Leitner, and M. Havenith, "An extended dynamical solvation shell around proteins," *Proc. Nat. Acad. Sci. USA*, vol. 104, no. 52, pp. 20 749–20 752, Dec. 2007.

[26] E. Bründermann, B. Born, S. Funkner, M. Krüger, and M. Havenith, "Terahertz spectroscopic techniques for the study of proteins in aqueous solutions," *Proc. SPIE*, vol. 7215, p. 72150E, 2009.

[27] K. Unterrainer, M. Helm, E. Gornik, E. E. Haller, and J. Leotin, "Mode structure of the p-germanium far-infrared laser with and without external mirrors: Single line operation," *Appl. Phys. Lett.*, vol. 52, pp. 564–566, 1988.

[28] S. Komiyama, H. Morita, and I. Hosako, "Continuous wavelength tuning of inter-valence-band laser oscillation in p-type germanium over range of $80 - 120$ μm," *Jpn. J. Appl. Phys.*, vol. 32, pp. 4987–4991, 1993.

[29] J. N. Hovenier, A. V. Muravjov, S. G. Pavlov, V. N. Shastin, R. C. Strijbos, and W. T. Wenckebach, "Active mode locking of a p-Ge hot hole laser," *Appl. Phys. Lett.*, vol. 71, pp. 443–445, 1997.

[30] A. V. Muravjov, R. C. Strijbos, C. J. Fredricksen, H. Weidner, W. Trimble, S. H. Withers, S. G. Pavlov, V. N. Shastin, and R. E. Peale, "Evidence for self-mode-locking in p-Ge laser emission," *Appl. Phys. Lett.*, vol. 73, pp. 3037–3039, 1998.

[31] J. N. Hovenier, R. M. De Kleijn, T. O. Klaassen, W. T. Wenckebach, D. R. Chamberlin, E. Bründermann, and E. E. Haller, "Mode-locked operation of the copper-doped germanium terahertz laser," *Appl. Phys. Lett.*, vol. 77, no. 20, pp. 3155–3157, Nov. 2000.

[32] P. F. Goldsmith, *Quasioptical Systems—Gaussian Beam Quasi-optical Propagation and Applications*. Piscataway, NJ: IEEE Press, 1998.

[33] B. Born, H. Weingärtner, E. Bründermann, and M. Havenith, "Solvation dynamics of model peptides probed by terahertz spectroscopy. observation of the onset of collective network motions," *J. Am. Chem. Soc.*, vol. 131, pp. 3752–3755, 2009.
[34] D. H. Auston, "Picosecond optoelectronic switching and gating in silicon," *Appl. Phys. Lett.*, vol. 26, pp. 101–103, 1975.
[35] K. Sakai and M. Tani, "Introduction to Terahertz Pulses," in *Terahertz Optoelectronics*. New York: Springer-Verlag, 2005, vol. 97, pp. 1–30.
[36] D. H. Auston, K. P. Cheung, and P. R. Smith, "Picosecond photoconducting Hertzian dipoles," *Appl. Phys. Lett.*, vol. 45, pp. 284–286, 1984.
[37] C. Janke, M. Först, M. Nagel, H. Kurz, and A. Bartels, "Asynchronous optical sampling for high-speed characterization of integrated resonant terahertz sensors," *Opt. Lett.*, vol. 30, no. 11, pp. 1405–1407, 2005.
[38] S. R. Tripathi, M. Aoki, K. Mochizuki, I. Hosako, T. Asahi, and N. Hiromoto, "Practical method to estimate the standard deviation in absorption coefficients measured with THz time-domain spectroscopy," *Opt. Commun.*, vol. 283, pp. 2488–2491, 2009.
[39] S. R. Tripathi, M. Aoki, K. Mochizuki, T. Asahi, I. Hosako, and N. Hiromoto, "Random error estimation in refractive index measured with the terahertz time domain spectroscopy," *IEICE Electron. Exp.*, vol. 6, no. 23, pp. 1690–1696, 2009.
[40] Z. G. Lu, P. Cambell, and X. C. Zhang, "Free-space electro-optic sampling with a high-repetion-rate regenerative amplified laser," *Appl. Phys. Lett.*, vol. 71, no. 5, pp. 593–595, 1997.
[41] P. U. Jepsen and B. M. Fischer, "Dynamic range in terahertz time-domain transmission and reflection spectroscopy," *Opt. Lett.*, vol. 30, no. 1, pp. 29–31, 2005.
[42] M. Van Exter and D. Grischkowsky, "Characterization of an optoelectronic terahertz beam system," *IEEE Trans. Microw. Theory Techn.*, vol. 38, no. 20, pp. 1684–1691, 1990.
[43] M. Naftaly and R. Dudley, "Methodologies for determining the dynamic ranges and signal-to-noise ratios of terahertz time-domain spectrometers," *Opt. Lett.*, vol. 34, pp. 1213–1215, 2009.
[44] M. Takeda, S. R. Tripathi, M. Aoki, and N. Hiromoto, "Exploration of the origin of random error in spectrum intensity measured with THz-TDS," in *Proc. 2010 35th Int. Conf. Infrared Millimeter and Terahertz Waves (IRMMW-THz)*, Sep. 2010, Paper Th-P. 58.

Heinz-Wilhelm Hübers received the diploma degree and the Dr. rer. nat. degree in physics in 1991 and 1994, respectively, from the Friedrich-Wilhelms Universität, Bonn, Germany.

From 1991 to 1994, he was with the Max-Planck-Institut für Radioastronomie, Bonn, Germany. In 1994 he joined Deutsches Zentrum für Luft- und Raumfahrt (DLR), Berlin, Germany, where he became head of Department of Experimental Planetary Physics in 2001. Since 2009, he has been a Professor of experimental physics at the Technische Universität Berlin and head of the Experimental Planetary Physics Department at DLR. His research interests are in THz physics and spectroscopy, particularly in THz systems for astronomy, planetary research, and security.

Prof. Hübers has received the Innovation Award on Synchrotron Radiation (2003) and the Lilienthal Award (2007).

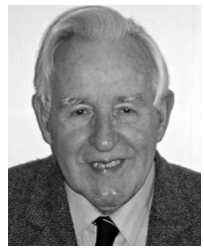

Maurice F. Kimmitt graduated from Trinity College, Dublin, Ireland, in 1954 and then joined the Radar Research Establishment, Malvern, U.K., where his initial studies were on semiconductors for infrared detection. In 1965 he moved to the University of Essex, Colchester, U.K., where he received the Ph.D. degree and wrote *Far-Infrared Techniques* (Pion Ltd, 1970).

In 1957 he joined a small group set up to study the far-infrared emission from ZETA, the U.K.'s first attempt at controlled fusion. This involved the development of new helium-cooled detectors and, later, the first FIR laser. In 1982 he "early retired" and has since then assisted with a variety of FIR/THz research projects in the UK, Italy, Germany, and at Dartmouth College.

Norihisa Hiromoto received the B.S. and Ph.D. degrees in physics from Kyoto University, Kyoto, Japan, in 1978 and 1985, respectively.

He joined the Communications Research Laboratory (CRL) in 1984 and his interests have included research on detector and laser technologies in the terahertz region and an asbestos fiber monitor using optical techniques. He became the director of Kansai Advanced Research Center of CRL in 2001 and moved to the Ministry of Public Management, Home Affairs, Posts and Telecommunications (MPHPT), as a Senior Planning Officer in 2003. Since 2005 he has been a professor at Shizuoka University, Hamamatsu, Japan. He has authored and co-authored more than 60 scientific and technical papers and holds four patents in terahertz and optical technology.

Erik Bründermann received the diploma and Dr. rer. nat. degrees in physics in 1991 and 1994, respectively, from the Friedrich-Wilhelms Universität, Bonn, Germany.

From 1989 to 1994, he was with the Max-Planck-Institut für Radioastronomie, Bonn, Germany. In 1994 he joined DLR, Berlin, Germany. In 1999 he became a member of the Ruhr-Universität Bochum. His research interests are in physics, mathematics, life science, and technology. He develops THz spectroscopy for liquid samples and IR chemical nanoscopes. In 2009, he was elected as Honorable Guest Professor at Shizuoka University, Hamamatsu, Japan. In 2010 he initiated the regional group "Ruhrgebiet" of the German Humboldt-Club. As group speaker he fosters exchange between scientists across faculties and disciplines.

He received a Feodor Lynen Award of the Humboldt-foundation joining the Lawrence Berkeley National Laboratory and the Center for Particle Astrophysics, Berkeley, CA in 1997 for two years.